

Gravitational lensing and the Sunyaev–Zel’dovich effect in the millimetre/submillimetre waveband

A. W. Blain

Cavendish Laboratory, Madingley Road, Cambridge, CB3 0HE.

26 June 2018

ABSTRACT

The intensity of the cosmic microwave background radiation in the fields of clusters of galaxies is modified by inverse Compton scattering in the hot intracluster gas – the Sunyaev–Zel’dovich (SZ) effect. The effect is expected to be most pronounced at a frequency of about 350 GHz (a wavelength of about 800 μm), and has been detected in the centimetre and millimetre wavebands. In the millimetre/submillimetre waveband, the gravitationally-lensed images of distant dusty star-forming galaxies in the background of the cluster are predicted to dominate the appearance of clusters on scales of several arcseconds, and could confuse observations of the SZ effect at frequencies greater than about 200 GHz (wavelengths shorter than about 1.5 mm). Recent observations by Smail, Ivison & Blain (1997) confirm that a significant population of confusing sources are present in this waveband. Previous estimates of source confusion in observations of the millimetre/submillimetre-wave SZ effect did not include the effects of lensing by the cluster, and so the accuracy of such measurements could be lower than expected. Source subtraction may be required in order to measure the SZ effect accurately, and a careful analysis of the results of an ensemble of SZ measurements could be used to impose limits to the form of evolution of distant dusty star-forming galaxies.

Key words: galaxies: clustering – galaxies: evolution – cosmic microwave background – cosmology: observations – gravitational lensing – radio continuum: galaxies

1 INTRODUCTION

Gravitational lensing can have a more significant effect on the population of galaxies detected in the millimetre/submillimetre waveband as compared with other wavebands; Blain (1996a,b; 1997a,b – Paper 1; 1997c, 1998) gives details of the effects of lensing by both galaxies and clusters. Here we consider the effects of the lensed images of background galaxies in millimetre/submillimetre-wave observations of clusters on arcminute angular scales that are suitable to detect the modifications to the intensity of the cosmic microwave background radiation (CMBR) due to the Sunyaev–Zel’dovich (SZ) effect (Sunyaev & Zel’dovich 1980; Rephaeli 1995b). Lensed images are not expected to be resolved on these scales, but they could produce significant source confusion because of their uncertain spatial distribution in the observing beam. Accurate estimates of this confusion could be necessary in order to interpret the results of observations of the SZ effect. The importance of source confusion in this waveband has recently been confirmed by the 850- μm observations of lensed images in the clusters Abell 370 and Cl2244–02 (Smail, Ivison & Blain 1997 – SIB). The effects of millimetre/submillimetre-wave

source confusion in the absence of gravitational lensing are discussed by Blain, Ivison & Smail (submitted – BIS).

The principal sources of millimetre/submillimetre-wave radiation from clusters are the SZ effect and the lensed images of distant dusty background galaxies. Other sources are star-forming or active galaxies within the cluster, the Rees–Sciama (RS) effect (Rees & Sciama 1968; Quilis, Ibáñez & Saez 1995) and primordial CMBR anisotropies. We discuss the properties and relative importance of all five sources in Section 2, and estimate the source confusion noise expected due to the lensed images of distant galaxies in Section 3. In Section 4 the consequences of this confusion for millimetre/submillimetre-wave observations of the SZ effect are discussed, and the prospects for using the same observations to detect the signature of galaxy evolution in the population of lensed images are assessed. Throughout this paper we assume that the density parameter $\Omega_0 = 1$ and that Hubble’s constant $H_0 = 50 \text{ km s}^{-1} \text{ Mpc}^{-1}$.

2 SOURCES OF MILLIMETRE/SUBMILLIMETRE-WAVE RADIATION IN CLUSTERS

2.1 The Sunyaev–Zel'dovich effect

The SZ effect describes the modifications to the spectrum of the CMBR due to inverse Compton scattering in the hot X-ray emitting gas bound to clusters of galaxies. It is usually separated into two components: a thermal effect, which describes the net energy gain of CMBR photons scattered by hot gas moving with the Hubble flow; and a kinematic effect, which describes the net Doppler shift of the photons scattered in a cluster with a non-zero peculiar velocity.

If the scattering gas is non-relativistic, then the thermal SZ effect produces a characteristic increment and decrement to the CMBR intensity above and below a frequency of 217 GHz respectively. The magnitude of this effect is independent of the redshift of the scattering gas and is determined by a single dimensionless parameter $y = \tau\sigma_T k_B T_e / (m_e c^2)$, in which τ is the scattering optical depth of the cluster and σ_T , T_e and m_e are the electron scattering cross section, temperature and mass respectively. The y -parameter is typically several times 10^{-4} in a rich cluster of galaxies (Rephaeli 1995b), and $|y| < 1.5 \times 10^{-5}$ over the whole sky (Fixsen et al. 1996). The magnitude of the kinematic SZ effect, which is expected to be smaller than the thermal SZ effect in a typical cluster, is proportional to τv_r , where v_r is the peculiar velocity of the scattering gas. If the scattering gas is relativistic, then the form of the thermal effect is no longer described completely by the y -parameter, and the values of both τ and T_e affect the spectrum of the CMBR independently (Rephaeli 1995a).

The spectrum of both the thermal and kinematic SZ effects expected for two clusters, both with $\tau = 10^{-2}$ and $v_r = 1000 \text{ km s}^{-1}$, are shown in Fig. 1. One cluster contains non-relativistic electrons with $k_B T_e < 5 \text{ keV}$ and has $y = 1.4 \times 10^{-4}$; the other contains relativistic electrons with $k_B T_e = 10 \text{ keV}$. Limits to the intensity of the diffuse extragalactic background radiation from the FIRAS instrument on the *COBE* satellite (Puget et al. 1996; Fixsen et al. 1996) are also shown.

The centimetre-wave SZ effect has been detected by Birkinshaw (1990), Uyaniker et al. (1997) and Myers et al. (1997) at frequencies of 20.3, 10.55 and 32 GHz respectively using single-antenna telescopes, and by Jones et al. (1993) and Carlstrom, Joy & Grego (1996) using interferometers at 15 and 30 GHz respectively. Recently, Grainge et al. (1996) produced the first image of the SZ effect at 15 GHz. In the millimetre waveband, the SZ decrement has been detected near the peak of the CMBR spectrum at 2.2 mm (Wilbanks et al. 1994), using the SuZIE bolometer array receiver at the Caltech Submillimeter Observatory (Holzapfel et al. 1997), and Andreani et al. (1996) have detected the SZ increment at 1.2 mm. Silverberg et al. (1997) recently detected the submillimetre-wave SZ effect in the direction of the Coma cluster at four frequencies but low significance using the MSAM balloon-borne experiment.

Current observations of the SZ effect are consistent with a cored isothermal surface brightness distribution, which depends on angular radius θ as $[1 + (\theta/\theta_c)^2]^{-1/2}$. The rich clusters Abell 2218 and Abell 2163 at redshifts $z_c = 0.171$ and 0.201 have core radii $\theta_c \simeq 50$ and 70 arcsec respectively (Squires et al. 1996; Elbaz, Arnaud & Böhringer 1995).

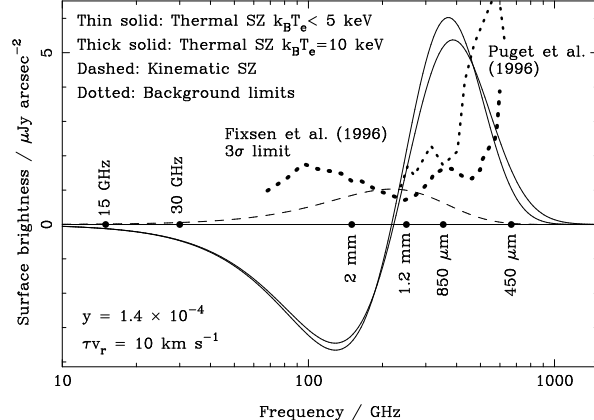


Figure 1. Predictions of the spectrum of the thermal and kinematic SZ effects in a typical rich cluster. The frequency of the peak in the CMBR spectrum is 160 GHz. Observed limits to the intensity of diffuse extragalactic background radiation and the frequencies of important observing bands are also shown.

2.2 Lensed images of background galaxies

The properties of the lensed images of distant dusty star-forming galaxies lensed by a rich cluster at a redshift $z_c = 0.17$ were discussed in Paper 1, and are expected to have flux densities in the range 1 to 10 mJy at 850 μm , comparable to or larger than the flux densities of any star-forming galaxies within the lensing cluster. Distant galaxies are expected to be relatively bright in the millimetre/submillimetre waveband because the K -corrections due to redshifting the dust emission spectra of distant galaxies are expected to be large and negative as compared with other wavebands (Blain & Longair 1993a). Hence, faint galaxies detected in the millimetre/submillimetre waveband are typically expected to have redshifts much larger than z_c , and so, even if z_c were increased substantially, a large surface density of background galaxies and lensed images would still be expected.

SIB have recently detected examples of such distant dusty galaxies in the fields of the clusters A370 and Cl2244-02 at $z_c = 0.37$ and 0.33 respectively. The surface density of these objects is larger than that predicted previously (Blain & Longair 1996), but is consistent with the observed background radiation intensity in the far-infrared waveband (Puget et al. 1996) and with recent observations of the Hubble Deep Field at a wavelength of 2.8 mm (Wilner & Wright 1997). Even in the absence of gravitational lensing these sources are expected to contribute a significant amount of confusion noise to some observations in the millimetre/submillimetre waveband (BIS).

2.3 Other sources of radiation

The far-infrared radiation emitted by dust in star-forming galaxies within a cluster could produce a detectable flux density in the submillimetre waveband. The fraction of blue star-forming galaxies in clusters tends to increase with increasing redshift, described as the Butcher–Oemler (BO) effect (Butcher 1978, Lavery & Henry 1994, Couch et al. 1994), and would correspond to an increase in the luminosity of these galaxies in the far-infrared waveband.

The Rees-Sciama (RS) effect is expected to produce a signal with a spectrum similar to that of the CMBR. If the density of the core of a cluster evolves during its light crossing time, then the gravitational blueshift imposed on a CMBR photon as it falls into the cluster is not matched by the gravitational redshift imposed as it climbs out, and so the spectrum of the CMBR is modified. Quilis, Ibáñez & Saez (1995) have calculated the largest possible signal due to this effect.

Gravitational lensing of primordial anisotropies in the CMBR would lead to a spatially-correlated millimetre/submillimetre-wave background signal on scales similar to the Einstein radius of the lensing cluster (Paper 1).

2.4 The relative importance of these sources

The frequency-dependent surface brightness of the SZ increment to the CMBR intensity in the core of a cluster with $y = 1.4 \times 10^{-4}$ should peak at about $6 \mu\text{Jy arcsec}^{-2}$ at a wavelength of about $850 \mu\text{m}$ (Fig. 1). In comparison, the largest values of surface brightness of resolved lensed images and galaxies in the cluster at $z_c = 0.171$ that was modeled in Paper 1 were about 60 and $6 \mu\text{Jy arcsec}^{-2}$ respectively. The RS effect and primordial CMBR anisotropies are expected to produce much smaller surface brightnesses of order 300 and $30 \text{nJy arcsec}^{-2}$ respectively at their maximum intensities (Paper 1).

The millimetre/submillimetre-wave flux densities of any dusty star-forming galaxies within a cluster are expected to be considerably smaller than those of the lensed images of distant galaxies unless the galaxies are in a cluster at a low redshift, that is if z_c is significantly less than 0.1 (Paper 1). The spectral energy distributions of distant lensed images should be flatter than those of cluster galaxies, and so at higher frequencies the cluster galaxies should be relatively brighter as compared with the lensed images; however, the lensed images are still expected to be brighter than the cluster galaxies throughout the millimetre/submillimetre waveband. The typical flux densities of the lensed images should approximately follow the envelope to the observed limits to the background radiation intensity shown in Fig. 2.

Lensed images are expected to dominate the appearance of clusters on arcsecond scales; however, on larger angular scales the surface brightness distribution of the SZ effect becomes more significant, and the SZ signal is expected to dominate in observations on arcminute scales at $850 \mu\text{m}$.

3 ESTIMATING SOURCE CONFUSION

3.1 Introduction

Source confusion is the uncertainty introduced into the results of an observation by the flux densities of unresolved sources that lie at unknown positions in the observing beam. Source confusion due to extrapolated and inferred populations of distant dusty galaxies has been estimated by Franceschini et al. (1989, 1991), Helou & Beichman (1990), Toffolatti et al. (1995) and Gawiser & Smoot (1997). BIS have recently made the first estimates to be based on the results of direct submillimetre-wave observations. Fischer &

Lange (1993) discussed the effects of unlensed source confusion on observations of the SZ effect, and estimated that the confusion noise at a wavelength of $850 \mu\text{m}$ in a 1-arcmin observing beam should be about 20 times smaller than the signal of the SZ effect from a cluster with $y = 10^{-4}$. BIS estimate that source confusion at $850 \mu\text{m}$ is actually about a factor of 7 times more severe than this earlier value.

Confusion noise in the field of a cluster should be increased by gravitational lensing, because both the mean separation and flux density of bright lensed images are expected to be larger than those of unlensed background galaxies. In the following sections we estimate the size of this increase and discuss its effects on observations of the SZ effect. In order to make an accurate measurement of the SZ effect, the flux densities of confusing sources may need to be subtracted from the observed signal. This is usually achieved by observing the cluster to the same limiting flux density but at a finer angular resolution, in order to detect the confusing galaxies while resolving out the SZ signal. Loeb & Refregier (1997) have shown that this procedure could introduce a subtle bias into measurements of the SZ effect. Because lensed images are typically brighter than unlensed galaxies, a larger fraction of their total number can be detected at any flux density limit as compared with unlensed galaxies. The images are expected to be more strongly magnified in the inner few arcminutes of the field of a cluster, and so source subtraction is expected to be more efficient there as compared with the outer regions of the field. It is this difference in efficiencies that introduces the systematic error into the SZ measurement. However, this effect is not of immediate concern in the millimetre/submillimetre waveband, because accurate source subtraction will be impossible in this waveband until large interferometer arrays are available (Brown 1996; Downes 1994, 1996). The current accuracy of millimetre-wave observations of the SZ effect is limited by the uncertain flux densities of all the confusing galaxies and not just by their incomplete subtraction.

3.2 The procedure

The effects of gravitational lensing on source confusion was estimated by combining several different models of galaxy evolution (Blain & Longair 1996) with a model of lensing by clusters (Paper 1). A large set of random distributions of background galaxies and their lensed images were derived, and their surface brightness distributions were convolved with Gaussian beams on various scales in order to produce distributions of the flux densities due to both lensed and unlensed sources in the beams. The widths of these distributions were then used to predict the source confusion noise expected with and without gravitational lensing.

3.2.1 Modeling galaxy formation and evolution

Three models of the evolution of the population of dusty star-forming galaxies are included in this paper; models I1 and I2 are based on pure luminosity evolution of the *IRAS* luminosity function (Saunders et al. 1990), and model H is based on a model of mergers in an hierarchical clustering scheme (Blain & Longair 1993a,b) that is derived from the Press-Schechter formalism (Press & Schechter 1974). The

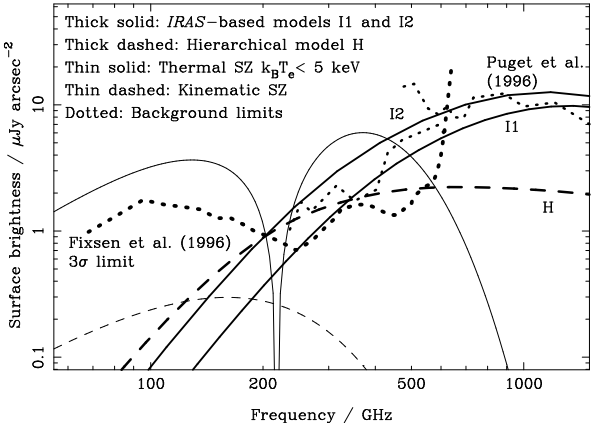


Figure 2. The predicted diffuse background intensities in three models of galaxy formation (Table 1), limits to the intensity of diffuse background emission and the spectrum of the SZ effect (Fig. 1). Note that the diffuse background intensities are much larger than the expected level of source confusion noise.

models are described in more detail by Blain & Longair (1996), in which model I1 was labelled model 3. In model I1 pure luminosity evolution is by a factor $(1+z)^3$ when $z \leq 2$ and by a factor 27 when $2 < z \leq 5$. In model I2, the $(1+z)^3$ form of evolution extends to a larger redshift $z = 2.6$, and the evolution factor is 46.7 when $2.6 < z \leq 7$. Model I2 was used to describe the observed counts of SIB. The background radiation intensities predicted by each model are shown in Fig. 2 and are consistent with the observed limits to the diffuse background radiation intensity (Puget et al. 1996; Fixsen et al. 1996).

3.2.2 Modeling the effects of lensing

A ray-tracing method for determining the distribution and properties of the lensed images of galaxies behind a cluster was demonstrated in Paper 1. A spherical model of a lensing cluster with properties similar to those of Abell 2218 was used (Natarajan & Kneib 1996); that is, with a velocity dispersion $\sigma_v = 1360 \text{ km s}^{-1}$ at a redshift $z_c = 0.171$ (Kneib et al. 1996). The effects that different values of σ_v and z_c have on the predicted source confusion are discussed in Section 3.4.

3.2.3 Combining the models

The source confusion with and without gravitational lensing was estimated from a large number of surface brightness distributions at chosen frequencies in the millimetre/submillimetre waveband, which were set up in 10-arcmin-wide fields using galaxies drawn at random from the luminosity functions describing the galaxy distribution expected in models I1, I2 and H above. The corresponding surface brightness distribution of the lensed images of these galaxies in each field were then determined using the lensing model. Each lensed and unlensed surface brightness distribution was then convolved with a set of Gaussian beams, with full-width-half-maximum (FWHM) beam-widths θ_b between 5 and 300 arcsec in order to produce val-

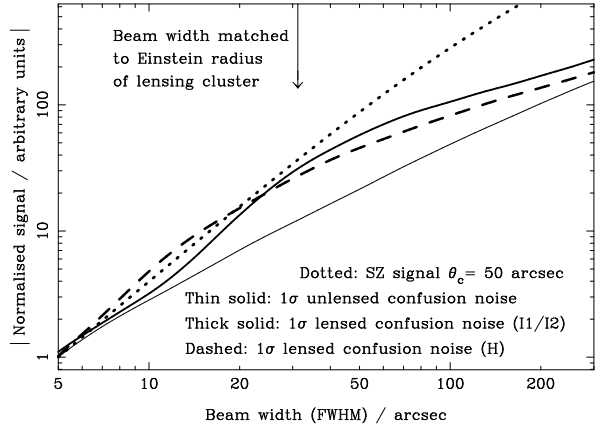


Figure 3. The relative amplitude of the 1σ confusion noise expected with and without lensing in a beam-switched observation of the SZ effect due to distant dusty star-forming galaxies as a function of beam-width. The predicted amplitudes are different in model H as compared with models I1 and I2. An arbitrarily-normalised SZ signal is also shown.

ues of the flux density of unresolved sources on each angular scale. After repeating this process many times the width of the resulting distributions of flux density values, $\sigma_1(\theta_b)$ and $\sigma_S(\theta_b)$ for lensed and unlensed sources respectively, were determined and used to estimate the confusion noise. These widths were defined as half the range of flux density that included 60 per cent of the simulated flux densities. Any difference in the mean flux density in the simulated lensed and unlensed fields gives an estimate of the residual signal expected due to lensing; this difference was always found to be smaller than σ_1 and σ_S .

The SZ effect can be detected by either making a fully-sampled image of the field of a cluster or in a ‘beam-switched’ observation that measures the differential signal between a beam that is centred on the core of the cluster and a reference beam that is offset by several beam-widths. The confusion noise expected in a beam-switched observation is given by the quadrature sum of the values of confusion noise in each beam, which are both given by σ_S if the effects of lensing are neglected, and by σ_1 and σ_S if lensing is included. In an imaging observation, estimates of confusion noise with and without lensing are given directly by σ_1 and σ_S respectively.

3.3 The results

The estimates of confusion noise presented here were derived from simulations in 240 random fields at wavelengths of 2 mm, 1.2 mm, 850 μm and 450 μm . The dependence of confusion noise on beam-width was found to be very similar at each wavelength; Fig. 3 shows the combined profile of the results at all four wavelengths, with and without lensing for model H and for models I1 and I2. A typical predicted profile of the SZ signal is also shown. The increase in source confusion due to gravitational lensing is most pronounced when the beam-width θ_b is matched to the Einstein radius of the lensing cluster θ_E , that is when $\theta_b \sim 2\theta_E$. In these calculations $\theta_E \simeq 16$ arcsec (Paper 1), and so source confu-

sion is predicted to increase most significantly, by a factor of about 3, at $\theta_b \simeq 32$ arcsec. The predicted increase in confusion is smaller in larger beams, and tends gradually to its unlensed value when $\theta_b \gg \theta_E$.

The modifications to the confusion noise due to lensing take this form because the most strongly magnified images are formed at angular radii close to θ_E ; most images at smaller radii are demagnified, and images at larger radii are magnified by progressively smaller amounts. In a beam smaller than the Einstein radius, lensing modifies the confusion noise slightly, but as θ_b increases towards $2\theta_E$, a steadily increasing fraction of the flux density from strongly magnified images at θ_E is included in the observing beam, and so the confusion noise increases. As θ_b increases above θ_E , the less strongly magnified images at radii larger than θ_E contribute a steadily increasing fraction of the detected flux density; therefore, the contribution of the strongly magnified images at radii near θ_E is steadily diluted, and so the confusion noise tends gradually to its unlensed value.

The confusion noise expected in each observing band and model of galaxy evolution is shown in Table 1 and Fig. 4. The results for beam-widths of 1 and 2 arcmin are presented in Table 1, while in Fig. 4 the results in a 1-arcmin beam are compared with earlier estimates. The estimates of unlensed confusion noise are significantly larger than those of Helou & Beichman (1990) and Fischer & Lange (1993), but are more similar to those of Franceschini et al. (1991). They are in good agreement with observationally-based estimates (BIS). Confusion noise is expected to dominate the SZ signal at a wavelength of $450\,\mu\text{m}$ and to be very significant at wavelengths of $850\,\mu\text{m}$ and $1.2\,\text{mm}$. In a 1-arcmin beam the lensed confusion noise is always predicted to be at least 20 per cent of the SZ signal in all three models. Only at a wavelength of $2\,\text{mm}$ is the SZ signal expected to be much larger than the confusion noise. These results suggest both that the kinematic SZ effect would be difficult to detect, and that the thermal SZ effect would be difficult to measure accurately, in an observation of a single cluster, unless the population of distant dusty star-forming galaxies is very sparse or evolves very weakly. In the light of recent observations (SIB) either of these scenarios appears very unlikely.

3.4 The mass and redshift of the lensing cluster

The key parameter that determines the effects of gravitational lensing on the confusion noise in an observation is the Einstein radius of the lensing cluster θ_E , which in turn depends on the redshift z_c , velocity dispersion σ_v and internal structure of the cluster. If the cluster is assumed to be an isothermal sphere, and $D(z, z_s)$ is the angular diameter distance between a redshift z and a source at redshift z_s , then $\theta_E \propto D(z_c, z_s)\sigma_v^2$ (Paper 1). Note that because z_s is typically much larger than unity for faint submillimetre-wave sources, increasing z_c does not significantly reduce the surface density of background sources, and so the only significant effect of changing z_c on the expected confusion due to lensed images is introduced through the resulting change in θ_E . The dependence of the SZ signal from an unresolved cluster on σ_v and z_c was discussed by De Luca, Désert & Puget (1995), using models of cluster evolution from Kaiser (1986) and Bartlett & Silk (1994), and found to take the form

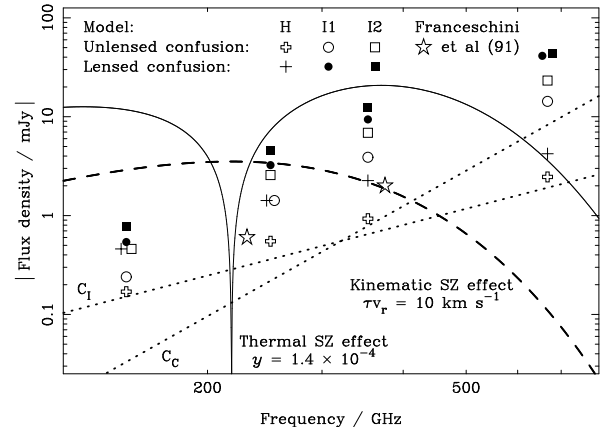


Figure 4. The $1-\sigma$ confusion noise expected in a beam-switched observation of the SZ effect with and without lensing in a 1-arcmin beam. The confusion estimates of Franceschini et al. (1991) and Fischer & Lange (1993; dotted lines) are also shown. C_C and C_I are estimates of the confusion due to galactic cirrus emission and *IRAS* galaxies respectively. C_I is very similar to the estimate of confusion noise in Helou & Beichman (1990).

$(1 + z_c)\sigma_v^{10/3}/D(0, z_c)^2$. A beam correction can be added to calculate the SZ signal expected from clusters that are resolved in smaller observing beams.

The expected dependence of both the confusion noise and the SZ signal at a wavelength of $850\,\mu\text{m}$ for clusters with $0.05 \leq z_c \leq 1$ and $800\,\text{km}\,\text{s}^{-1} \leq \sigma_v \leq 2000\,\text{km}\,\text{s}^{-1}$ is shown in Figs 5(a) & 5(b) for model I1. The results are normalised to match the predictions for the model lensing cluster in the previous sections, which had $z_c = 0.171$ and $\sigma_v = 1360\,\text{km}\,\text{s}^{-1}$. The confusion noise is expected to be smaller and larger by a factor of a few in models H and I2 respectively. Confusion noise is expected to be less significant as compared with the SZ signal in observations of more massive and more distant clusters that are made in larger beams, as shown by the signal-to-noise ratios in Figs 5(c) & 5(d).

4 CONFUSION NOISE AND OBSERVATIONS

4.1 Existing observations

Three ground-based detections of the millimetre-wave SZ effect have been published; for Abell 2163 at a wavelength of $2.2\,\text{mm}$ in a 1.4-arcmin-wide beam (Wilbanks et al. 1994), and for Abell 2744 and S1077 at wavelengths of 2 and $1.2\,\text{mm}$ in 46- and 44-arcsec-wide beams respectively (Andreani et al. 1996). The detected flux densities and estimates of the source confusion noise in these observations are listed in Table 2.

Silverberg et al. (1997) observed the Coma cluster at four frequencies using MSAM, a balloon-borne experiment, to search for the submillimetre-wave SZ effect. Because of the 28-arcmin beamwidth in this experiment, gravitational lensing will have an insignificant effect on the confusion noise in this observation. They estimate that CMBR fluctuations at an intensity $\Delta T/T \simeq 2 \times 10^{-5}$ would be a significant source of confusion in this observation. Distant dusty galax-

Table 1. Estimates of the 1σ confusion noise expected for SZ measurements due to lensed and unlensed background galaxies. The y -parameter and core radius of the cluster are assumed to be 1.4×10^{-4} and 50 arcsec respectively. The estimates are uncertain to within about 10 per cent.

Frequency / GHz (Wave- length / μm)	FWHM beam / arcsec	SZ signal / mJy	1- σ confusion noise: lensed (unlensed) / mJy			Ratio of SZ signal to confusion noise: lensed (unlensed)		
			Model I1	Model I2	Model H	Model I1	Model I2	Model H
150 (2000)	60	-11.7	0.54 (0.24)	0.77 (0.46)	0.46 (0.17)	22 (49)	15 (25)	25 (69)
	120	-36.3	0.93 (0.54)	1.48 (0.90)	0.78 (0.36)	39 (68)	25 (40)	47 (100)
250 (1200)	60	7.32	3.24 (1.42)	4.51 (2.57)	1.42 (0.55)	2.3 (5.2)	1.6 (2.9)	5.2 (13)
	120	22.7	5.58 (3.13)	8.79 (5.23)	2.42 (1.14)	4.1 (7.3)	2.6 (4.3)	9.4 (20)
350 (850)	60	20.5	9.39 (3.89)	12.4 (6.88)	2.26 (0.93)	2.2 (5.3)	1.7 (3.0)	9.1 (22)
	120	63.6	16.0 (8.56)	24.6 (14.3)	3.94 (1.98)	4.0 (7.4)	2.6 (4.4)	16 (32)
670 (450)	60	3.61	41.3 (14.3)	44.0 (23.2)	4.22 (2.46)	0.09 (0.25)	0.08 (0.16)	0.86 (1.5)
	120	11.2	66.6 (31.9)	90.5 (49.1)	7.96 (5.76)	0.17 (0.35)	0.12 (0.23)	1.4 (1.9)

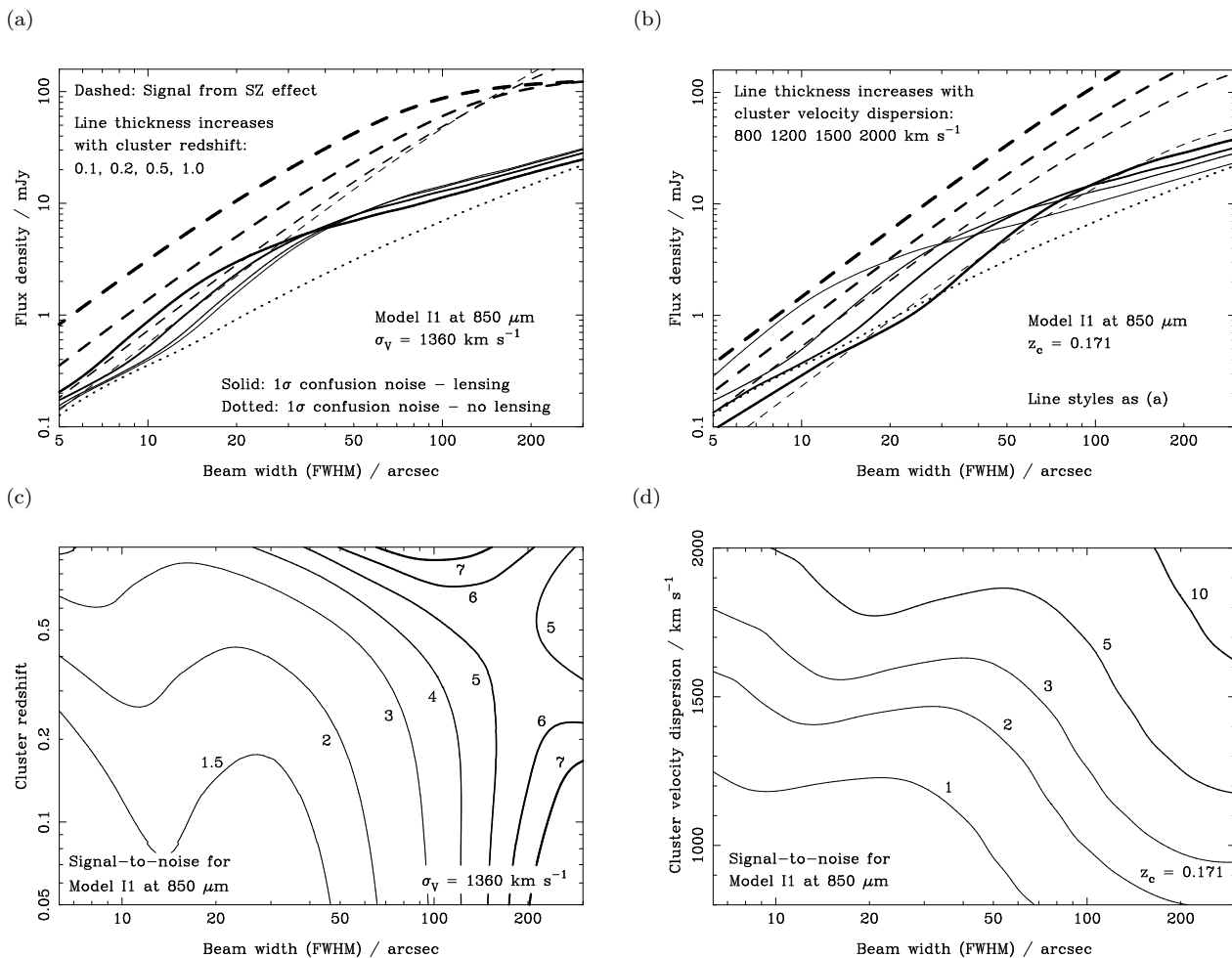


Figure 5. The effects of the redshift z_c and velocity dispersion σ_v of a cluster on the SZ signal and source confusion noise expected at 850 μm in model I1. The properties of the clusters are normalised to match the model described in Section 3.2.2, which was similar to A2218 with $\sigma_v=1360 \text{ km s}^{-1}$ and $z_c=0.171$. The SZ signal and confusion noise as a function of beam-width for a cluster at $z_c=0.1, 0.2, 0.5$ and 1 are shown in (a); in (b) the same quantities are shown for a cluster with $\sigma_v=800, 1200, 1500$ and 2000 km s^{-1} . The ratio of the SZ signal to the confusion noise expected for a range of values of z_c and σ_v are shown in (c) and (d) respectively.

ies are expected to contribute a significant amount of confusion noise in only the highest frequency channel, equivalent to $\Delta T/T \simeq 4 \times 10^{-5}$ at 678 GHz (BIS).

A2163 lies at a redshift $z_c=0.201$, has a core radius $\theta_c \simeq 70$ arcsec (Elbaz, Arnaud & Böhringer 1995), and $\sigma_v=1680 \text{ km s}^{-1}$ (Markevitch et al. 1996). If the

mass profile of A2163 is assumed to be scaled from that of A2218, then these observations indicate an Einstein radius $\theta_E \simeq 24$ arcsec, which leads to the estimates of confusion noise listed in Table 2. Hence, although we expect lensing to increase the level of source confusion noise in this observation, it should not exceed about 1 per cent of the

detected SZ signal in this cluster. Upgraded versions of the SuZIE instrument used in this observation (Holzapfel et al. 1997) continue to offer excellent performance for detecting the millimetre/submillimetre-wave SZ effect.

The SZ signals listed in Table 2 for A2744 and S1077, at redshifts $z_c = 0.308$ and 0.312 respectively, are derived from the y -parameters quoted by Andreani et al. (1996), and depend only weakly on the assumed core radii of these clusters. The differential signal from this beam-switched observation would be smaller by about 30 to 40 per cent due to the signal from the SZ effect that remains in the reference beams 135 arcsec away on the sky. Estimates of the Einstein radii of A2744 and S1077 are required in order to determine the confusion noise expected in these observations. The temperatures of 7 keV quoted for the intracluster gas in both A2744 and S1077 match that of A2218 (Squires et al. 1996). Hence, if self-similar cluster evolution is valid (Kaiser 1986), then $\theta_E \simeq 13$ arcsec for both clusters. However, the temperature of 12 keV has recently been determined for A2744 (Mushotzky & Scharf 1997), in which case $\theta_E \simeq 26$ arcsec. The values of confusion noise that are predicted assuming values of $\theta_E \simeq 13$ and 26 arcsec for S1077 and A2744 respectively are listed in Table 2. These values are greater than about 1 and 10 per cent of the SZ signal at wavelengths of 2 and 1.2 mm respectively in all three models of galaxy evolution. In models I1 and I2 the unlensed source confusion at a wavelength of 1.2 mm is expected to be several times larger than the value of 0.4 mJy suggested by Andreani et al. (1996). A further increase in confusion noise due to bright lensed images in the reference beam is very unlikely, because the reference beams are separated by 135 arcsec from the cluster core.

We expect the confusion noise in existing observations of the millimetre-wave SZ effect to be about 1 and 10 per cent of the SZ signal at wavelengths of about 2 mm and 1.2 mm respectively, and so these detections are unlikely to be artifacts of confusion noise. If a large number of detections of the SZ effect could be obtained at 1.2 mm then a careful analysis of the sources of noise could be used to estimate the amount of source confusion present, and so limit the form of evolution of distant dusty galaxies. Observations at several wavelengths would assist this analysis, as the amplitude of the confusing signal at each wavelength should be correlated for each cluster.

4.2 Future observations

A range of new instruments and telescopes could detect the millimetre/submillimetre-wave SZ effect. Suitable space-borne instruments include ESA's *Far InfraRed and Submillimetre Telescope (FIRST)*, a 3.5-m submillimetre-wave/far-infrared telescope (Pilbratt 1997), and *Planck Surveyor* (formerly *COBRAS/SAMBA*; Bersanelli et al. 1996), a CMBR imaging satellite with a $1.5 \text{ m} \times 1.292 \text{ m}$ aperture. Suitable ground-based instruments include the SCUBA camera at the James Clerk Maxwell Telescope (Cunningham et al. 1994), the US-Mexican 50-m Large Millimetre Telescope (LMT) (Cortes-Medellin & Goldsmith 1994) and large millimetre interferometer arrays (MIAs; Downes 1994). Observations by balloon-borne experiments, such as MSAM (Silverberg 1997) and BOOMERANG (Lange et al. 1995), are also capable of detecting the submillimetre-wave SZ effect. How-

Table 2. Estimates of source confusion noise in existing observations of the SZ effect (Wilbanks et al. 1994; Andreani et al. 1996). The results are derived in Section 4.1. The observing wavelength λ and reported SZ signal S_{SZ} are also listed.

Cluster	$\lambda /$ mm	$S_{\text{SZ}} /$ mJy	1- σ confusion noise:			
			lensed (unlensed) / mJy	Model I1	Model I2	Model H
A2163	2.2	-68	0.75 (0.36)	1.04 (0.60)	0.65 (0.25)	
A2744	2.0	-19	0.33 (0.18)	0.41 (0.32)	0.34 (0.13)	
	1.2	13	1.80 (0.96)	2.27 (1.75)	1.00 (0.38)	
S1077	2.0	-26	0.41 (0.18)	0.58 (0.32)	0.36 (0.13)	
	1.2	18	2.34 (0.96)	3.16 (1.75)	1.06 (0.38)	

ever, these instruments have beamwidths of order several tens of arcminutes and so the effects of gravitational lensing are unimportant. Applicable estimates of unlensed source confusion for these experiments can be found in BIS.

4.2.1 FIRST

At present, the longest observing wavelength of *FIRST*'s bolometer instrument is $500 \mu\text{m}$ (Griffin 1997), and so the instrument's spectral range is not optimized to detect the peak of the signal due to the SZ effect at a wavelength of about $800 \mu\text{m}$ (Fig. 1). *FIRST*'s angular resolution is finer than about 40 arcsec at $500 \mu\text{m}$, and so any observations of the SZ effect are likely to be affected by source confusion. The expected flux density from the core of a cluster with $y = 10^{-4}$ in a 40-arcsec beam is about 4 mJy, as compared with estimated lensed and unlensed 1σ source confusion noise values of at least 6 and 2 mJy beam^{-1} in model I1, Fig. 5(a). *FIRST* should reach a 1σ sensitivity limit of about 1 mJy beam^{-1} at $500 \mu\text{m}$ in a 25-arcmin^2 field in a 6-hour integration (Griffin 1997), and so a detection would be possible in a reasonable integration time in the absence of source confusion. However, without resolving and subtracting the flux density from confusing sources obtaining a reliable detection for an individual cluster using *FIRST* would be difficult.

4.2.2 Planck Surveyor

In a 1-year all-sky survey *Planck Surveyor* should detect the SZ effect in about 1.5×10^4 clusters with $y > 8 \times 10^{-5}$ and core radii subtending about 1 arcmin (Bersanelli et al. 1996). The kinematic SZ signal of the brighter clusters in the sample could be used to determine their peculiar velocities to an accuracy of about 100 to 300 km s^{-1} (Haehnelt & Tegmark 1996). Similar predictions have recently been made by Aghanim et al. (1997). A $1.5 \text{ m} \times 1.292 \text{ m}$ aperture corresponds to a beam-width of about 3 arcmin at $850 \mu\text{m}$, and so gravitationally lensed source confusion is not expected to degrade the performance of *Planck Surveyor* by a large amount (Fig. 5). The unlensed confusion noise expected for *Planck Surveyor* is discussed by BIS: in the 353-GHz channel, in which the thermal SZ signal is expected to be largest, a 1σ noise level of about 12 mJy is expected in each 19-arcmin^2 pixel. The nominal 1σ sensitivity of the *Planck* survey is comparable, at $16 \text{ mJy pixel}^{-1}$ (Bersanelli et al. 1996).

4.2.3 SCUBA

In a 30-hour integration in a 10-arcmin² field SCUBA should be able to detect point sources with flux densities of about 7 and 40 mJy at a signal to noise ratio of 3σ , given the currently attainable sensitivities (SIB, JCMT web page). These sensitivities match the thermal SZ signal from the core of clusters with y -parameters of 8.4×10^{-4} and 0.12 at 850 and 450 μm respectively. SCUBA could hence detect a cluster with $y = 1.4 \times 10^{-4}$ at a signal to noise ratio of about 0.5σ beam⁻¹ at the centre of the field at 850 μm ; however, the cluster could not be detected at 450 μm . The resulting 850- μm map with an angular resolution of about 13 arcsec would contain about 200 resolution elements. The surface brightness of the SZ signal would still have 40 per cent of its central value at the edge of the field if $\theta_c \simeq 50$ arcsec, and so the signal to noise ratio for the thermal SZ effect in the observation would be about 3σ . The corresponding kinematic effect would not be detectable, reaching a signal-to-noise ratio of only 0.5 if $\tau v_r = 10 \text{ km s}^{-1}$. In general, an observation of a 10-arcmin² field lasting t hours should detect the thermal SZ effect from a cluster with $\theta_c \simeq 50$ arcsec at a signal to noise ratio of about $0.4[y/10^{-4}]t^{1/2}$. In a fixed integration time, the signal to noise ratio for an observation of the SZ effect in a circular field centred on the cluster is maximized when the radius of the field is twice that of the cluster core.

SCUBA will allow limited source subtraction of the brightest lensed images in the field, as discussed in Paper 1 and recently confirmed by SIB. However, confusion noise from fainter images could still be significant. In order to subtract a larger fraction of lensed images and reduce the confusion noise, observations using either the LMT, with an angular resolution limit of about 5 arcsec at a wavelength of 1 mm, or a large MIA, with sub-arcsecond resolution, would be required.

4.2.4 Millimetre interferometer arrays

The performance of large MIAs (Downes 1994) was discussed in Paper 1 in the context of detecting lensed images in the fields of clusters. The large collecting areas and very sensitive receivers of these instruments will allow very faint images to be detected at sub-arcsecond angular resolution. However, the instantaneous field-of-view of a large interferometer is limited to the primary beam area of its individual antennas, which is about 0.4 arcmin² for an array of 8-m antennas at a wavelength of 1.3 mm, and so observations of fields that are several arcminutes in extent would require the accurate mosaicing (Cornwell 1992) of many different fields. A mosaic of about 25 primary beam areas would be required in order to make the most sensitive detection of the SZ effect at 850 μm from a cluster with $\theta_c \simeq 50$ arcsec in a 9-arcmin² field. Fewer mosaiced fields would be required at longer wavelengths, for which the primary beam area is larger. At a wavelength of 3 mm the primary beam area of an array of 8-m antenna would be about 2 arcmin², and so a mosaic of only 5 beams would be required to map the cluster. Hence, the most efficient strategy to detect the SZ effect using an MIA would probably be to observe in the millimetre rather than the submillimetre waveband.

In a compact array configuration, the proposed Large

Southern Array (Downes 1996) should be able to map a 9-arcmin² field down to a 3σ sensitivity of about 0.13 mJy in each 10-arcsec² synthesised beam at a wavelength of 1.3 mm in a 4-hour integration. The Millimeter Array (Brown 1996) and Large Millimetre and Submillimetre Array (Ishiguro et al. 1992) should offer a similar performance. An MIA could hence detect the brightest lensed images in a rich cluster in a matter of hours, and would be ideal for carrying out sensitive source subtraction in the millimetre/submillimetre waveband. If an MIA is assumed to have a constant point source sensitivity, then the flux density limit at any wavelength can be estimated by scaling the value given above at 1.3 mm by the areas of the primary and synthesized beams at other wavelengths. In this case, the thermal SZ effect from a cluster with $y = 1.4 \times 10^{-4}$ and $\theta_c = 50$ arcsec could be detected by an MIA with signal-to-noise ratios of about 40, 15, 2 and 6σ in 1-hour integrations at wavelengths of 3, 2, 1.3 and 0.85 mm respectively. An MIA could hence obtain a very significant detection of the millimetre-wave SZ effect. Confusing sources could be subtracted accurately using observations on longer baselines, and so a very detailed image of the millimetre-wave SZ effect could be produced.

5 CONCLUSIONS

The effects of the lensed images of distant dusty star-forming galaxies on observations of the SZ effect in the millimetre/submillimetre waveband, in which distant sources are intrinsically bright have been discussed. Such images have recently been detected by Smail et al. (1997).

(i) Gravitational lensing of distant galaxies is expected to increase source confusion noise in millimetre/submillimetre-wave observations of the SZ effect. The most pronounced increase, by a factor of about 3, is expected in observing beams that are matched to the Einstein radius of the lensing cluster. This increased estimate of confusion noise is not sufficiently large to affect the interpretation of existing millimetre-wave observations of the SZ effect; however, it could provide a significant source of noise in future observations on arcminute scales, and the brightest sources may need to be subtracted in order to measure the SZ effect accurately.

(ii) The effect of gravitational lensing on confusion noise in the fields of clusters depends on both the form of the population and evolution of distant star-forming galaxies, and the surface density of the lensing cluster. In general, a larger signal-to-noise ratio would be obtained from an observation of a more massive cluster, at a larger redshift, in an observing beam that is several times larger than the Einstein radius of the cluster.

(iii) Future millimetre/submillimetre-wave observations of the SZ effect using ground-based and space-borne instruments will be affected by confusion in different ways. The angular resolution of *Planck Surveyor* is probably sufficiently coarse to avoid significantly increased source confusion due to lensing in clusters. Observations using telescopes with smaller beams, such as *FIRST* and ground-based single-antenna telescopes, will be more seriously affected. Large millimetre interferometer arrays will be very valuable instruments for carrying out source subtraction and will be able

to detect the SZ effect directly, most easily in the millimetre waveband.

ACKNOWLEDGEMENTS

I would like to thank Alastair Edge for his prompt refereeing of this paper, and Malcolm Longair for useful discussions during its preparation.

REFERENCES

Aghanim N., De Luca A., Bouchet F. R., Gispert R., Puget J.-L., 1997, *A&A*, 325, 9

Andreani P. et al., 1996, *ApJ*, 459, L49

Bartlett J. G., Silk J., 1994, *ApJ*, 423, 12

Bersanelli M. et al., 1996, COBRAS/SAMBA Phase A Study Report, D/SCI(96)3 ESA

Birkinshaw M., 1990, in Mandolesi N., Vittorio N. eds. *The Cosmic Microwave Background: 25 Years Later*, Kluwer, Dordrecht, p. 77

Blain A. W., 1998, *MNRAS*, in press; astro-ph/9710160

Blain A. W., 1997a, in Holt S. S., Mundy J. G., eds, *Star formation: near and far*, AIP, Woodbury NY, p.606

Blain A. W., 1997b, *MNRAS*, 290, 553; Paper 1

Blain A. W., 1997c, in Wilson A. ed, *The far-infrared and submillimetre universe*, vol. SP-401, ESA, Noordwijk, p. 175; astro-ph/9710139

Blain A. W., 1996a, *MNRAS*, 283, 1340

Blain A. W., 1996b, in Shaver P. ed., *Science with large millimetre arrays*, Springer-Verlag, Berlin, p. 75

Blain A. W., Longair M. S., 1996, *MNRAS*, 279, 847

Blain A. W., Longair M. S., 1993a, *MNRAS*, 264, 509

Blain A. W., Longair M. S., 1993b, *MNRAS*, 265, L21

Blain A. W., Ivison R. J., Smail I., *MNRAS*, submitted; astro-ph/9710003; BIS

Brown R. L., 1996, in Bremer M. N. et al. eds, *Cold Gas at High Redshift*, Kluwer, Dordrecht, p. 411

Butcher H., 1978, *ApJ*, 219, 18

Carlstrom J. E., Joy M., Grego L., 1996, *ApJ*, 456, L75

Cornwell T. J., 1992, in Ishiguro M., Welch W. J. eds, *Astronomy with millimeter and submillimeter interferometry*, PASP conference series, vol. 59, p. 96

Cortes-Medellin G., Goldsmith P. F., 1994, *IEEE Trans. Antennas Propagation*, 42, 176

Couch W. J., Ellis R. J., Sharples R. M., Smail I., 1994, *ApJ*, 430, 121

Cunningham C. R., Gear W. K., Duncan W. D., Hastings P. R., Holland W. S., 1994, *Instrumentation in Astronomy VIII*. Proc. SPIE, vol. 2198, 638

De Luca A., Désert F.-X., Puget J.-L., 1995, *A&A*, 300, 335

Downes D., 1994, in Wamsteker W., Longair M. S., Kondo Y. eds, *Astronomy with Millimeter and Submillimeter Wave Interferometry*, Kluwer, Dordrecht, p. 133

Downes D., 1996, in Shaver P. ed., *Science with Large Millimetre Arrays*, Springer-Verlag, Berlin, p. 16

Elbaz D., Arnaud M., Böhringer H., 1995, *A&A*, 293, 337

Fischer M. L., Lange A. E., 1993, *ApJ*, 419, 433

Fixsen D. J., Cheng E. S., Gales J. M., Mather J. C., Shafer R. A., Wright E. L., 1996, *ApJ*, 473, 576

Franceschini A., Toffolatti L., Mazzei P., Danese L., De Zotti G., 1991, *A&AS*, 89, 285

Franceschini A., Toffolatti L., Mazzei P., Danese L., De Zotti G., 1989, *ApJ*, 344, 35

Gawiser E., Smoot G. F., 1997, *ApJ*, 480, L1

Grainge K., Jones M., Pooley G., Saunders R., Baker J., Haynes T., Edge A., 1996, *MNRAS*, 278, L17

Griffin M. J., 1997, in Wilson A. ed, *The far-infrared and submillimetre universe*, vol. SP-401, ESA, Noordwijk, p. 31

Haehnelt M. G., Tegmark M., 1996, *MNRAS*, 279, 545

Helou G., Beichman C. A., 1990, in Kaldeich B. ed., *From ground-based to space-borne sub-millimetre astronomy*. ESA vol. 314, p. 117, ESA publications

Holzapfel W. L., Wilbanks T. M., Ade P. A. R., Church S. E., Fischer M. L., Mauskopf P. D., Osgood D. E., Lange A. E., 1997, *ApJ*, 479, 17

Ishiguro M., Kawabe R., Nakai N., Morita K.-I., Okumura S. K., Ohashi N., 1992, in Ishiguro M., Welch W. J. eds, *Astronomy with millimeter and submillimeter interferometry*, PASP conference series, vol. 59, p. 405

JCMT web page, 1997, http://www.jach.hawaii.edu/~wsh/scuba/scuba_home.html

Jones M. et al., 1993, *Nat*, 365, 320

Kaiser N., 1986, *MNRAS*, 222, 323

Kneib J.-P., Ellis R. S., Smail I., Couch W. J., Sharples R. M., 1996, *ApJ*, 471, 643

Lange A. E. et al., 1995, *Space Science Reviews*, 74, 145

Lavery R. J., Henry J. P., 1994, *ApJ*, 426, 524

Loeb A., Refregier A., 1997, *ApJ*, 476, L59

Markevitch M., Mushotzky R., Inoue H., Yamashita K., Furuzawa A., Tawara Y., 1996, *ApJ*, 456, 437

Mushotzky R. F., Scharf C. A., 1997, *ApJ*, 482, L13

Myers S. T., Baker J. E., Readhead A. C. S., Leitch E. M., Herbig T., 1997, *ApJ*, 485, 1

Natarajan P., Kneib J.-P., 1996, *MNRAS*, 283, 1031

Pilbratt G., 1997, in Wilson A. ed, *The far-infrared and submillimetre universe*, vol. SP-401, ESA, Noordwijk, p. 7

Press W. H., Schechter P., 1974, *ApJ*, 187, 425

Puget J.-L., Abergel A., Bernard J.-P., Boulanger F., Burton W. B., Désert F.-X., Hartmann D., 1996, *A&A*, 308, L5

Quilis V., Ibáñez J. M., Saez D., 1995, *MNRAS*, 277, 445

Rees M. J., Sciama D. W., 1968, *Nat*, 217, 511

Rephaeli Y., 1995a, *ApJ*, 445, 33

Rephaeli Y., 1995b, *ARA&A*, 33, 541

Saunders W., Rowan-Robinson M., Lawrence A., Efstathiou G., Kaiser N., Ellis R. S., Frenk C. S., 1990, *MNRAS*, 242, 318

Silverberg R. F. et al., 1997, *ApJ*, 485, 22

Smail I., Ivison R. J., Blain A. W., 1997, *ApJ*, 490, L5; astro-ph/9708135; SIB

Squires G., Kaiser N., Babul A., Fahlman G., Woods D., Neumann D. M., Böhringer H., 1996, *ApJ*, 461, 572

Sunyaev R. A., Zel'dovich Ya. B., 1980, *ARA&A*, 18, 537

Toffolatti L. et al., 1995, *Astron. Lett. and Comm.*, 32, 125

Uyaniker B., Reich W., Schlickeiser R., Wielebinski R., 1997, *A&A*, 325, 516

Wilbanks T. M., Ade P. A. R., Fischer M. L., Holzapfel W. L., Lange A. E., 1994, *ApJ*, 427, L75

Wilner D. J., Wright M. C. H., 1997, *ApJ*, 488, L67